Letter

Rectification and nonlinear Hall effect by fluctuating finite-momentum Cooper pairs

Akito Daido* and Youichi Yanase
Department of Physics, Graduate School of Science, Kyoto University, Kyoto 606-8502, Japan

(Received 21 February 2023; accepted 1 March 2024; published 9 April 2024)

Nonreciprocal charge transport is attracting much attention as a novel probe and functionality of noncentrosymmetric superconductors. In this work we show that both the longitudinal and the transverse nonlinear paraconductivity are hugely enhanced in helical superconductors under moderate and high magnetic fields, which can be observed by second-harmonic resistance measurements. The discussion is based on the generalized formulation of nonlinear paraconductivity in combination with the microscopically determined Ginzburg-Landau coefficients. The enhanced nonreciprocal transport would be observable even with the cyclotron motion of fluctuating Cooper pairs, which is elucidated with a Kubo-type formula of the nonlinear paraconductivity. Nonreciprocal charge transport in the fluctuation regime is thereby established as a promising probe of helical superconductivity regardless of the sample dimensionality. Implications for the other finite-momentum superconducting states are briefly discussed.

DOI: 10.1103/PhysRevResearch.6.L022009

Introduction. Nonreciprocal charge transport (NCT) is attracting much attention as the novel functionality of noncentrosymmetric materials [1–35]. An example is a diodelike material property known as magnetochiral anisotropy (MCA), which refers to directional resistance, or rectification, linear in the magnetic field and has been observed in a variety of materials [3–9]. Unidirectional transport even with zero and finite resistance has also been realized, namely, the superconducting diode effect (SDE) [10–22]. The nonlinear Hall effect (NHE) is another hot topic [24–29], by which a finite transverse resistance can be produced in time-reversal symmetric materials. These findings pave the way for next-generation devices [9,17,18,30,31]. Furthermore, NCT would serve as a versatile electrical probe of inversion-symmetry breaking, applicable even under extreme conditions including high pressure and magnetic fields. Thus, NCT phenomena are hallmarks of modern condensed-matter physics.

The development of NCT techniques may shed light on the fascinating phenomena of noncentrosymmetric superconductors that are hardly captured via conventional experiments. Among other things, helical superconductivity [36–47] is a long-sought finite-momentum superconducting state, regardless of its predicted ubiquity in magnetic fields. The pair potential of helical superconductivity has a plane-wave expression known as the Fulde-Ferrell type [48] without the modulation of amplitude. This makes its experimental identification more difficult than the Larkin-Ovchinnikov and pair-density-wave states [49–52], whose detection has been reported via spatially resolved techniques in various superconductors [53–62] including FeSe [57], Sr_2RuO_4 [58], $Bi_2Sr_2CaCu_2O_{8+\delta}$ [59,60], CsV_3Sb_5 [61], and UTe_2 [62]. Recent theoretical studies [20,22,63] have revealed that the characteristic crossover phenomenon of helical superconductivity can be signaled by the sign reversal of the SDE, offering a promising probe free of Josephson junctions in contrast to the known methods [41,64]. Further investigation of NCT would provide us with keys to understanding exotic superconducting states in noncentrosymmetric systems.

The disadvantage of the SDE as a probe of helical superconductivity is to require small-width samples to suppress vortex motion and approach the depairing limit of the critical current [65]. It has also been pointed out that the SDE is sensitive to the conditions around sample edges [66,67]. Thus, careful microfabrication would be required to study the intrinsic SDE in candidate helical superconductors such as heavy-fermion superlattices [68,69] and thin films of Pb [70] and $SrTiO_3$ [71]. Toward easier access to helical superconductivity, we turn renewed attention to the nonreciprocal paraconductivity, i.e., NCT by fluctuating Cooper pairs, which is little affected by the edge environments. In pioneering works [6,32,33], nonreciprocal paraconductivity was studied focusing on MCA and was shown to be significantly larger than MCA of normal electrons [6]. The theoretical studies not only succeeded in explaining the experiment in MoS_2 [6], but also pointed out that spin-singlet and -triplet mixing of Cooper pairs can be detected [32,33]. However, their formulation is not applicable in the presence of finite-momentum Cooper pairs and/or nonlinear effects of the magnetic field, leaving helical superconductors out of its scope.

In this Letter, we generalize the previous formulation of nonreciprocal paraconductivity and show that the rectification and NHE in the fluctuation regime are hugely enhanced in helical superconductors in moderate and strong magnetic fields. We also show that the enhanced NCT would still

*daido@scphys.kyoto-u.ac.jp

be observable even in the presence of the cyclotron motion of Cooper pairs. Our formulation is applicable to Fulde-Ferrell-type superconducting states in general, while thin-film Larkin-Ovchinnikov superconductors may also be explored by applying symmetry-breaking perturbations. Our results showcase an interesting example of NCT that originates from the intrinsic nature of exotic Cooper pairs.

Notation for NCT. We begin by introducing the notation for rectification and the NHE, which is described by the nonlinear conductivity $j_i = \sigma_1^{ij} E_j + \sigma_2^{ijk} E_j E_k$ or the nonlinear resistivity $E_i = \rho^{ij} j_j = \rho_1^{ij} j_j + \rho_2^{ijk} j_j j_k$. Here linear and nonlinear resistivities satisfy $\rho_1 = \sigma_1^{-1}$ and

$$\rho_2^{ijk} = -\left[\sigma_1^{-1}\right]_{ia} \sigma_2^{abc} \left[\sigma_1^{-1}\right]_{bj} \left[\sigma_1^{-1}\right]_{ck}. \tag{1}$$

The nonlinear resistivity can be observed via the longitudinal and Hall second-harmonic resistance [5]. The nonlinear resistivity ρ_2^{xxx} gives rise to nonreciprocity in the longitudinal resistivity ρ^{xx} in the electric current j_x,

$$\rho^{xx} = \rho_1^{xx}(1 + \eta^{xxx} j_x), \quad \eta^{xxx} \equiv \rho_2^{xxx}/\rho_1^{xx}. \tag{2}$$

The longitudinal nonreciprocity η^{xxx} is a natural generalization of the γ value for MCA [1,2] and is used as a quantitative measure of rectification in this paper: According to Eq. (2), its inverse $1/\eta^{xxx}$ gives a typical current density for nonreciprocity to be visible. We also introduce

$$\eta^{xyy} \equiv \rho_2^{xyy}/\rho_1^{xx} \tag{3}$$

to compare the NHE with rectification and call it Hall nonreciprocity, although the linear Hall effect vanishes in the model studied later.

Near the transition temperature T_c of superconductors, the conductivity tends to diverge due to the fluctuation of Cooper pairs, which interpolates the finite and vanishing resistance in normal and superconducting states [72]. The linear and nonlinear conductivities σ_1 and σ_2 can be decomposed into those in the normal state and the excess contribution by fluctuation which are specified by the subscripts n and s, respectively: $\sigma_1 = \sigma_{1n} + \sigma_{1s}$ and $\sigma_2 = \sigma_{2n} + \sigma_{2s}$. Our purpose is to obtain the paraconductivity contributions σ_{1s} and σ_{2s} and thereby evaluate the nonlinear resistivities ρ^{xxx} and ρ^{xyy} in the fluctuation regime of superconductors.

Time-dependent Ginzburg-Landau theory. Let us consider a d-dimensional superconductor slightly above T_c, with $d = 2$ unless specified otherwise. Following Refs. [6,32,33], we study the fluctuation of Cooper pairs by using the phenomenological time-dependent Ginzburg-Landau (GL) equation in the momentum space [73],

$$\Gamma_0 \frac{\partial \psi_{\boldsymbol{q}}(t)}{\partial t} = -\alpha_{\boldsymbol{q}} \psi_{\boldsymbol{q}}(t) + \zeta_{\boldsymbol{q}}(t), \tag{4a}$$

$$\langle \zeta_{\boldsymbol{q}}^*(t) \zeta_{\boldsymbol{q}'}(t') \rangle = \frac{2\Gamma_0 T}{V} \delta(t - t') \delta_{\boldsymbol{q},\boldsymbol{q}'}, \tag{4b}$$

with the GL functional $F[\psi] = V \sum_{\boldsymbol{q}} \alpha_{\boldsymbol{q}} |\psi_{\boldsymbol{q}}|^2$. The random force $\zeta_{\boldsymbol{q}}(t)$ is assumed to be the white noise as in the second line and reproduces $\langle |\psi_{\boldsymbol{q}}|^2 \rangle = T/V\alpha_{\boldsymbol{q}}$ in equilibrium. The effect of the electric field $\boldsymbol{E}$ is introduced by $\alpha_{\boldsymbol{q}} \to \alpha_{\boldsymbol{q}-2\boldsymbol{A}(t)}$, with $\boldsymbol{A}(t) = -\boldsymbol{E}t$. The excess current density by fluctuating Cooper pairs is evaluated with the formula [6,73,74]

$$\begin{aligned} \boldsymbol{j}_s &= \lim_{t\to\infty} -\sum_{\boldsymbol{q}} \partial_{\boldsymbol{A}} \alpha_{\boldsymbol{q}-2\boldsymbol{A}(t)} \langle |\psi_{\boldsymbol{q}}(t)|^2 \rangle \\ &= \frac{4T}{\Gamma_0} \int \frac{d^d q}{(2\pi)^d} \partial_{\boldsymbol{q}} \alpha_{\boldsymbol{q}} \int_{-\infty}^{0} dt_1 \exp\left(-\frac{2}{\Gamma_0} \int_{t_1}^{0} dt' \alpha_{\boldsymbol{q}-2\boldsymbol{A}(t')} \right), \end{aligned} \tag{5}$$

which results from a process where Cooper pairs are formed by fluctuations and then accelerated by the electric field until they vanish after a finite lifetime.

Within the GL picture, the superconducting transition is triggered by the softening of the mode $\boldsymbol{q} = \boldsymbol{q}_0$, which minimizes $\alpha_{\boldsymbol{q}}$. This occurs at $\boldsymbol{q}_0 \neq 0$ in helical superconductivity, in contrast to $\boldsymbol{q}_0 = 0$ in conventional superconductors. Note that the modes around $\boldsymbol{q}_0$ dominantly contribute to transport properties in the vicinity of T_c. Thus, we can expand the GL coefficient in terms of $\delta\boldsymbol{q} = \boldsymbol{q} - \boldsymbol{q}_0$,

$$\begin{aligned} \alpha_{\boldsymbol{q}} &= \alpha_{\boldsymbol{q}_0} + \alpha_2^{ij} \delta q_i \delta q_j + \alpha_3^{ijk} \delta q_i \delta q_j \delta q_k + O(\delta q^4) \\ &\equiv N_0 \left(\epsilon + \sum_i \xi_i^2 \delta q_i^2 + \bar{\xi}^3 \sum_{ijk} \mathcal{A}^{ijk} \delta q_i \delta q_j \delta q_k \right). \end{aligned} \tag{6}$$

We defined the reduced temperature $\epsilon \equiv (T - T_c)/T$, the GL coherence length ξ_i and its geometric mean $\bar{\xi} \equiv (\prod_{i=1}^d \xi_i)^{1/d}$, and the dimensionless third-rank tensor $\mathcal{A}^{ijk}$, while the overall coefficient $N_0 \equiv T \frac{\partial}{\partial T} \alpha_{\boldsymbol{q}_0}$ is related to the density of states. Importantly, cubic anharmonicity $\mathcal{A}^{ijk}$ is allowed with $\boldsymbol{q}_0 \neq 0$ and/or without both inversion and time-reversal symmetries.

Nonlinear paraconductivity. The GL formula of the fluctuation conductivity can be obtained by plugging Eq. (6) into Eq. (5) and expanding it by the electric field $\boldsymbol{E}$. We neglect the orbital magnetic field for the time being, while the effect of the Zeeman field can be taken into account. The linear fluctuation conductivity is then given by $L_z \sigma_{1s}^{ij} = \frac{\tau_0 T}{2\pi\epsilon} \frac{\xi_i^2}{\xi_x \xi_y} \delta_{ij}$ to the leading order of the reduced temperature ϵ, with the sample thickness L_z and the GL relaxation time $\tau_0 \equiv \Gamma_0/N_0 > 0$ [72,73,75]. In the absence of anisotropy, this reproduces $L_z \sigma_{1s} = 1/16\epsilon$ for $\tau_0 = \pi/8T$ [72].

The nonlinear paraconductivity is similarly obtained [73],

$$L_z \sigma_{2s}^{ijk} = \frac{\tau_0^2 T \sqrt{\xi_x \xi_y}}{4\pi\epsilon^2} \mathcal{A}^{ijk}, \tag{7}$$

to the leading order of the reduced temperature ϵ. The NCT is of $O(\epsilon^{-2})$, as reported previously [6,32,33]. Notably, it is the anharmonicity parameter $\mathcal{A}^{ijk}$ that gives rise to NCT [6,33], since $\boldsymbol{q}_0$ can be traced out from Eq. (5) by shifting the momentum. Note that σ_{2s}^{ijk} allows not only rectification but also the NHE. Nonlinear paraconductivities for system dimensions $d = 1$ and 3 are also obtained as $L_y L_z \sigma_{2s}^{xxx} = \frac{3\tau_0^2 T \xi_x^2}{8\epsilon^{5/2}} \mathcal{A}^{xxx}$ and $\sigma_{2s}^{ijk} = \frac{\tau_0^2 T}{16\pi\epsilon^{3/2}} \mathcal{A}^{ijk}$, respectively, where $L_y L_z$ is the wire cross section. We emphasize that the obtained formulas allow us to discuss the nonlinear effect of the Zeeman field $\boldsymbol{h}$ and, if any, coexisting time-reversal-breaking orders, in contrast to the previous formulas showing $O(h)$ NCT in specific

TABLE I. Typical forms of $\boldsymbol{g}_{\mathcal{A}}(\hat{n}) = \boldsymbol{g}_{\mathcal{A}}(\delta\boldsymbol{q})/\delta q^3$ and $\frac{\partial}{\partial\theta}\boldsymbol{g}_{\mathcal{A}}(\hat{n})$ for various types of antisymmetric SOC. Here we define $\delta\boldsymbol{q} = \delta q\,\hat{n}$ and unit vectors $\hat{n} = (\cos\theta, \sin\theta, 0)$ and $\hat{z} = (0, 0, 1)$.

Type of SOC	$\boldsymbol{g}_{\mathcal{A}}(\hat{n})$	$\frac{\partial}{\partial\theta}\boldsymbol{g}_{\mathcal{A}}(\hat{n})$
Rashba	$\hat{z}\times\hat{n}$	$-\hat{n}$
chiral	$\hat{n}$	$\hat{z}\times\hat{n}$
Ising	$\sin 3\theta\,\hat{z}$	$3\cos 3\theta\,\hat{z}$
Dresselhaus	$\sin 2\theta\,\hat{z}\times\hat{n}$	$2\cos 2\theta\,\hat{z}\times\hat{n} - \sin 2\theta\,\hat{n}$

two-dimensional models [6,32,33]. This point is crucial to describe fluctuating finite-momentum Cooper pairs.

To illustrate the formula (7), we discuss NCT linear in the Zeeman field $\boldsymbol{h}$ before studying the nonlinear effects of $\boldsymbol{h}$. In this case, the anharmonicity parameter $\mathcal{A}^{ijk}$ is $O(h)$ and can be rewritten in the form of the cubic spin-orbit coupling (SOC) [63]

$$\mathcal{A}^{ijk}\delta q_i\delta q_j\delta q_k \equiv \boldsymbol{h}\cdot\boldsymbol{g}_{\mathcal{A}}(\delta\boldsymbol{q}). \tag{8}$$

The effect of $\boldsymbol{h}$ on the other coefficients is $O(h^2)$ and thus is negligible in the low-field region. For the purpose of symmetry considerations, the effective SOC $\boldsymbol{g}_{\mathcal{A}}(\delta\boldsymbol{q})$ can be identified with the antisymmetric SOC of the system around the Γ point in the Brillouin zone [63]. Typical forms of the effective SOC in Rashba, chiral, Ising, and Dresselhaus systems are illustrated with a unit vector $\hat{n}$ in Table I. When the electric field with strength E is applied in an in-plane direction $\hat{E}$, the $O(E^2)$ excess current density $\delta^2\boldsymbol{j}_{\rm s}$ in this direction is $\hat{E}\cdot\delta^2\boldsymbol{j}_{\rm s} \propto \mathcal{A}^{ijk}\hat{E}_i\hat{E}_j\hat{E}_k$ from Eq. (7), i.e., $\hat{E}\cdot\delta^2\boldsymbol{j}_{\rm s} \propto \boldsymbol{h}\cdot\boldsymbol{g}_{\mathcal{A}}(\hat{E})$. The field-angle dependence of rectification is determined by the effective SOC $\boldsymbol{g}_{\mathcal{A}}(\hat{E})$ (Table I). Similarly, the transverse excess current density is given by $(\hat{z}\times\hat{E})\cdot\delta^2\boldsymbol{j}_{\rm s} \propto \boldsymbol{h}\cdot\frac{\partial}{\partial\theta}\boldsymbol{g}_{\mathcal{A}}(\hat{E})$ [73]. Here the θ derivative acts on $\hat{E} = (\cos\theta, \sin\theta, 0)$ and thus

$$(\hat{z}\times\hat{E})\cdot\delta^2\boldsymbol{j}_{\rm s} \propto \hat{E}\cdot\boldsymbol{h}, \tag{9}$$

e.g., in Rashba systems (Table I). This indicates that the NHE occurs for the magnetic field parallel to the electric field in contrast to the rectification that occurs in the perpendicular configuration. The results obtained here give the generalized and convenient description of the known results for the Rashba [32,33,73] and Ising systems [6,33].

It should be noted that the nonlinear resistivity ρ_2 rather than conductivity σ_2 is directly observed in experiments. It turns out that not only the linear resistivity ρ_1 but also the nonlinear resistivity ρ_2 vanishes as it approaches the transition temperature $\epsilon \to 0$ in the present framework, due to approximately σ_1^{-3} in Eq. (1). Nevertheless, the nonlinear resistivity ρ_2 can be hugely enhanced in the fluctuation regime before it finally vanishes, reflecting the divergence of the nonlinear conductivity σ_2. To estimate the nonlinear longitudinal and Hall resistivities ρ_2^{xxx} and ρ_2^{xyy} in the fluctuation regime, we define the reduced temperature ϵ_* indicating the linear-resistance drop by 25% of the normal-state value [73]. We denote the nonlinear resistivities evaluated at $\epsilon = \epsilon_*$ by ρ_{2*}^{xxx} and ρ_{2*}^{xyy}.

In contrast to the nonlinear resistivity, the nonreciprocity of the resistivities η^{xxx} and η^{xyy} in Eqs. (2) and (3) converges

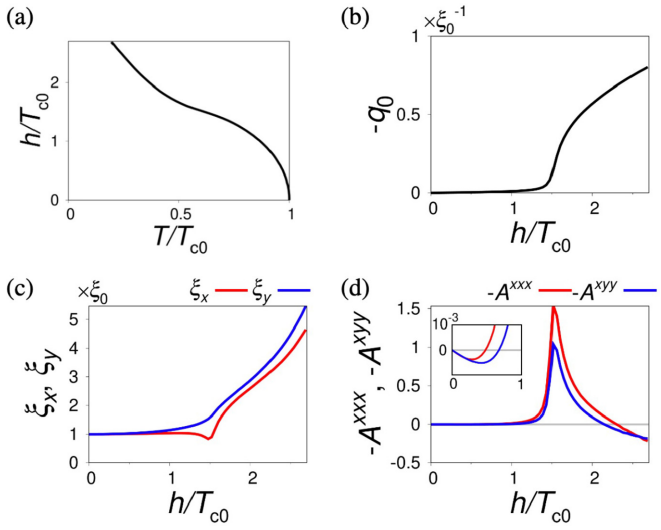

FIG. 1. (a) Transition line $(T_{\rm c}(h), h)$ of the s-wave Rashba-Zeeman superconductor, (b) Cooper-pair momentum $-q_0$, (c) GL coherence lengths ξ_x and ξ_y, and (d) anharmonicity parameters $-\mathcal{A}^{xxx}$ and $-\mathcal{A}^{xyy}$ along the transition line $(T_{\rm c}(h), h)$. Here ξ_x, ξ_y, and q_0^{-1} are in units of ξ_0, i.e., ξ_x and ξ_y at $h = 0$. The increasing tendency in ξ_x and ξ_y comes from the decrease of $T_{\rm c}(h)$. The inset in (d) shows the region $0 \leqslant h/T_{\rm c0} \leqslant 1$.

to a finite value as it approaches the transition temperature [6,32,33]. We define this limiting value by

$$\eta_{\rm s}^{ijk} \equiv \lim_{\epsilon\to+0}\eta^{ijk}(\epsilon) = -L_z\frac{\pi\sqrt{\xi_x\xi_y}}{T}\left(\frac{\xi_x\xi_y}{\xi_j\xi_k}\right)^2\mathcal{A}^{ijk} \tag{10}$$

for two-dimensional superconductors. This quantity measures the intrinsic nonreciprocity, which does not depend on the normal-state resistivity.

Application to helical superconductivity. By using the GL formula (7), we study rectification and the NHE in atomically thin s-wave and d-wave Rashba superconductors in the in-plane Zeeman field $\boldsymbol{h}$. The Bloch Hamiltonian is given by $H_N(\boldsymbol{k}) = \xi(\boldsymbol{k}) + [\boldsymbol{g}(\boldsymbol{k}) - \boldsymbol{h}]\cdot\boldsymbol{\sigma}$, with the hopping energy $\xi(\boldsymbol{k}) = -2t(\cos k_x + \cos k_y) - \mu$ and Rashba SOC $\boldsymbol{g}(\boldsymbol{k}) = \alpha_{\rm R}(-\sin k_y, \sin k_x, 0)$. We microscopically determine the GL coefficient $\alpha_{\boldsymbol{q}}$ [73], which gives $\boldsymbol{q}_0 = q_0\hat{x}$ upon minimization and ξ_i and $\mathcal{A}^{ijk}$ by taking $\boldsymbol{q}$ derivatives. The qualitative results do not depend on model parameters t, μ, $\alpha_{\rm R}$, etc., when $\alpha_{\rm R} \gg T_{\rm c0}$, as is the case in most noncentrosymmetric superconductors. Note that the Rashba energy $\alpha_{\rm R}$ is always dominant over the Zeeman energy h on the entire phase diagram since $h \sim T_{\rm c0}$ is considered. Here we denote the transition temperature in the magnetic field h by $T_{\rm c}(h)$ and $T_{\rm c0} \equiv T_{\rm c}(0)$. The parameters adopted for numerical calculations are available in the Supplemental Material [73].

We show in Fig. 1 the superconducting transition line and GL coefficients of the s-wave state. The Cooper-pair momentum q_0 of the soft mode along the transition line $(T_{\rm c}(h), h)$ is shown in Fig. 1(b), whose finite value indicates the realization of helical superconductivity for $T < T_{\rm c}(h)$. It is shown for $h/T_{\rm c0} \sim 1.5$ that the system experiences a rapid increase in $|q_0|$ known as the crossover between weakly and strongly helical states [36,37]. While the coherence lengths ξ_x and

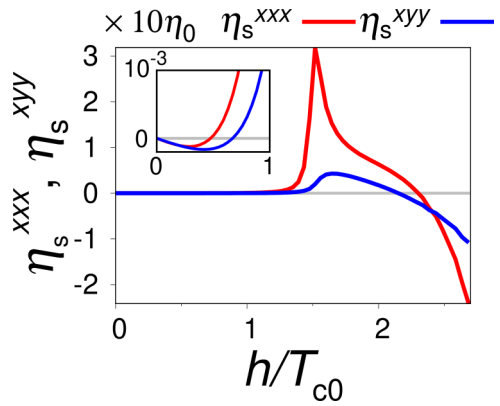

FIG. 2. Strength of the rectification $\eta_{\rm s}^{xxx}$ and NHE $\eta_{\rm s}^{xyy}$ in the s-wave Rashba-Zeeman superconductor along the transition line $(T_{\rm c}(h), h)$. The inset shows the region $0 \leqslant h/T_{\rm c0} \leqslant 1$.

ξ_y are always of the same order of magnitude [Fig. 1(c)], the anharmonicity parameters $\mathcal{A}^{xxx}$ and $\mathcal{A}^{xyy}$ are extremely enhanced in the crossover region as shown in Fig. 1(d): The rapid change in $\boldsymbol{q}_0$ naturally accompanies the anomalous $\boldsymbol{q}$ dependence of $\alpha_{\boldsymbol{q}}$ around there. The inset shows that $\mathcal{A}^{xxx}$ and $\mathcal{A}^{xyy}$ have tiny linear slopes corresponding to MCA in the small magnetic field h, as expected. The h-linear behavior is limited to the low-field region and thus the nonlinear effects are essential. The high-field behavior is discussed below. The huge increase of the anharmonicity parameters naturally enhances rectification and the NHE as shown in Fig. 2: Both the longitudinal and Hall nonreciprocities $\eta_{\rm s}^{xxx}$ and $\eta_{\rm s}^{xyy}$ given in Eq. (10) are increased by several orders of magnitude along the transition line. The enhancement of $\eta_{\rm s}^{xxx}$ compared to $\eta_{\rm s}^{xyy}$ originates from the increased anisotropy ξ_y/ξ_x in the crossover region [see Fig. 1(c) and Eq. (10)]. Similar results are obtained for various parameters and for the d-wave states [73]. The values of $\eta_{\rm s}^{ijk}$ obtained are comparable in units of $\eta_0 \equiv L_z\xi_0/T_{\rm c0}$, implying large NCT in superconductors with small $T_{\rm c0}$ and large ξ_0. For the case of heavy-fermion superlattices [69], we obtain $\eta_{\rm s}^{xxx} \sim 10\eta_{\rm s}^{xyy} \sim 10^{-2}$ μm^2/μA while assuming $\xi_0 \sim 5$ nm, $T_{\rm c0} \sim 2$ K, and $L_z \sim 10$ nm. This means that 10% rectification is obtained for a current density of approximately 10 μA/μm^2 at the mean-field transition temperature. Typical values of the nonlinear resistivity in the fluctuation regime are estimated to be $\rho_{2*}^{xxx} \sim 10\rho_{2*}^{xyy} \sim 10^{-4}$ Ω μm^3/μA while assuming $\sigma_{\rm 1n}^{-1} \sim 5 \times 10^{-7}$ Ω m. These values are well within the experimental scope. Thus, a sharp increase of rectification and the NHE in the crossover regime, as opposed to the standard h-linear behavior, serves as a promising probe of helical superconductivity.

Interestingly, the anharmonicity parameters take slightly smaller but still sizable values in higher magnetic fields [$h/T_{\rm c0} \gtrsim 2.5$ in Fig. 1(d)]. A large rectification and NHE are obtained there in combination with small $T_{\rm c}(h)$ (Fig. 2), while the sign reversal seen in Fig. 2 may be absent or shifted to higher fields, depending on model parameters [73]. It is known that the high-field helical superconductivity resembles in nature the Fulde-Ferrell-Larkin-Ovchinnikov (FFLO) state of centrosymmetric superconductors [37]. While these systems do not show nonreciprocal paraconductivity due to the cancellation of fluctuating Cooper pairs with opposite momenta, our results imply that the FFLO state, and possibly the pair-density-wave states, might show giant NCT once the symmetry-protected degeneracy of Cooper-pair momenta is externally lifted. This could be achieved by the out-of-plane bias voltage and in-plane magnetic field, realizing the same symmetry configurations as helical superconductivity. Quantitative studies are awaited for candidate materials such as cuprate thin films [52,76–79].

Orbital magnetic field. We have pointed out that a colossal rectification and NHE are promising probes of thin-film helical superconductors. A natural question is then whether the conclusion still holds in quasi-two-dimensional superconductors where the cyclotron motion of fluctuating Cooper pairs takes place. To study this problem, we derive a Kubo-type formula of $\sigma_{2\rm s}^{ijk}$ for the time-dependent GL equation of the form $\Gamma_0 \frac{\partial}{\partial t} |\psi(t)\rangle = \hat{\alpha} |\psi(t)\rangle + |\zeta(t)\rangle$,

$$\sigma_{2\rm s}^{ijk} = \frac{2\Gamma_0^2}{\beta V} \sum_{\mu\nu\lambda} \frac{J_{\mu\nu\lambda}^{ijk}(\alpha_\mu + \alpha_\nu + 2\alpha_\lambda)}{\alpha_\lambda(\alpha_\mu + \alpha_\nu)(\alpha_\mu + \alpha_\lambda)^2(\alpha_\nu + \alpha_\lambda)^2}, \tag{11}$$

with $\hat{\alpha} |\mu\rangle = \alpha_\mu |\mu\rangle$, $J_{\mu\nu\lambda}^{ijk} = {\rm Re}(\langle\mu|j_i|\nu\rangle \langle\nu|j_j|\lambda\rangle \langle\lambda|j_k|\mu\rangle)$, and $j_i = -\partial_{A_i}\hat{\alpha}$ [73]. This general formula of the phenomenological nonlinear paraconductivity is applicable to, e.g., systems with orbital magnetic fields as well as multiple pairing channels.

Let us consider bulk noncentrosymmetric superconductors in the magnetic field B in the y direction, which can be described by $\hat{\alpha} = \alpha_{\boldsymbol{q}}|_{\boldsymbol{q}\to\nabla/i-2\boldsymbol{A}(\boldsymbol{x})}$ [33,72,80]. We focus on the first-order effect of the anharmonicity parameters $\mathcal{A}^{xxx}$ and $\mathcal{A}^{xyy}$ for the purpose of an order estimate of NCT [73], $\sigma_{2\rm s}^{xxx} = \frac{\tau_0^2 T}{2\pi|\mathcal{B}|\sqrt{\bar{\epsilon}}}\mathcal{A}^{xxx}$ and $\sigma_{2\rm s}^{xyy} = \frac{3\tau_0^2 T}{4\pi\bar{\epsilon}^{3/2}}\mathcal{A}^{xyy}$, where $\mathcal{B} \equiv B\xi_x\xi_z$ is the magnetic flux threading the area spanned by the coherence length. The most singular terms regarding the reduced temperature in the magnetic field $\bar{\epsilon} \equiv \epsilon + 2|\mathcal{B}| = [T - T_{\rm c}(B)]/T$ are kept here, while $\sigma_{2\rm s}^{yxy} = \sigma_{2\rm s}^{yyx} = \sigma_{2\rm s}^{xyy}/2$ is obtained to the leading order of $\bar{\epsilon}$. The obtained nonlinear conductivity indicates that the orbital magnetic field suppresses the singularity of rectification perpendicular to the field while leaving that of the NHE intact [see the $d = 3$ result shown below Eq. (7)]. See Supplemental Material for more details of NCT for the orbital magnetic field.

The obtained expressions of NCT are proportional to the anharmonicity parameter $\mathcal{A}^{ijk}$, implying that the rapid increase of NCT occurs in bulk samples as well, triggered by the helical-superconductivity crossover. To estimate the nonreciprocity in the fluctuation regime, we discuss a typical value of nonreciprocity $\eta_*^{xxx} \equiv \rho_{2*}^{xxx}/\rho_{1*}^{xx}$ since the intrinsic limiting value $\eta_{\rm s}^{xxx}$ vanishes. At the reduced temperature defined by $\sigma_{\rm 1s}^{xx}(\bar{\epsilon}_*) = \sigma_{\rm 1n}^{xx}/3$, we obtain the nonreciprocity $\eta_*^{xxx} \sim 10^{-5}$ μm^2/μA for layered helical superconductors in the crossover region, by using the coherence lengths $\xi_x \sim \xi_y/2 \sim 5$ nm and $\xi_z \sim 2$ nm, relaxation time $\tau_0 \sim \pi/8T$, and $B \sim 2T_{\rm c0} \sim 0.4$ meV, as well as $\mathcal{A}^{xxx}$ estimated from Fig. 1(d). The NHE can be estimated similarly [73]. The obtained rectification and NHE $\rho_{2*}^{xxx} \sim \rho_{2*}^{xyy} \sim 10^{-5}$ Ω μm^3/μA are smaller than those of two-dimensional systems but are still observable when the fluctuation regime is visible for the experimental resolution of temperature [81].

Discussion. We have demonstrated that rectification and the NHE in the fluctuation regime are promising probes of helical superconductivity regardless of sample dimensions. The results strongly suggest that the enhanced NCT in moderate and high magnetic fields is observable in realistic thin-film samples with a non-negligible thickness, which would lie between the two-dimensional and three-dimensional limits studied in this work. In particular, the NHE would serve as a better probe because the linear Hall resistance is absent owing to the y-mirror symmetry. A materials-based study for the candidate helical superconductors [68–71] is left as an intriguing future issue, as well as the fully microscopic treatment of NCT including the quantum-mechanical corrections beyond the GL approach.

As a complementary question, it is also interesting to consider the effect of helical-superconductivity crossover on NCT caused by vortices and antivortices. This occurs below the mean-field transition temperature, and nonreciprocal renormalization of the superfluid density plays an essential role [33]. Since the anharmonicity parameter $\mathcal{A}^{ijk}$ causes such a renormalization, an enhanced NCT is also expected by this mechanism and would smoothly connect with that of paraconductivity above the mean-field transition temperature. Thus, the enhanced NCT in the crossover regime, both below and above the mean-field transition temperature, will work as the promising probe of helical superconductivity. Quantitative studies are left as a future issue.

Acknowledgments. We appreciate inspiring discussions with Yuji Matsuda and Tomoya Asaba. We are also grateful for helpful discussions with Hikaru Watanabe. This work was supported by JSPS KAKENHI (Grants No. JP18H01178, No. JP18H05227, No. JP20H05159, No. JP21K13880, No. JP21K18145, No. JP22H01181, No. JP22H04476, and No. JP22H04933) and SPIRITS 2020 of Kyoto University.

[1] Y. Tokura and N. Nagaosa, Nonreciprocal responses from non-centrosymmetric quantum materials, Nat. Commun. **9**, 3740 (2018).

[2] T. Ideue and Y. Iwasa, Symmetry breaking and nonlinear electric transport in van der Waals nanostructures, Annu. Rev. Condens. Matter Phys. **12**, 201 (2021).

[3] G. L. J. A. Rikken, J. Fölling, and P. Wyder, Electrical magnetochiral anisotropy, Phys. Rev. Lett. **87**, 236602 (2001).

[4] G. L. J. A. Rikken and P. Wyder, Magnetoelectric anisotropy in diffusive transport, Phys. Rev. Lett. **94**, 016601 (2005).

[5] T. Ideue, K. Hamamoto, S. Koshikawa, M. Ezawa, S. Shimizu, Y. Kaneko, Y. Tokura, N. Nagaosa, and Y. Iwasa, Bulk rectification effect in a polar semiconductor, Nat. Phys. **13**, 578 (2017).

[6] R. Wakatsuki, Y. Saito, S. Hoshino, Y. M. Itahashi, T. Ideue, M. Ezawa, Y. Iwasa, and N. Nagaosa, Nonreciprocal charge transport in noncentrosymmetric superconductors, Sci. Adv. **3**, e1602390 (2017).

[7] F. Qin, W. Shi, T. Ideue, M. Yoshida, A. Zak, R. Tenne, T. Kikitsu, D. Inoue, D. Hashizume, and Y. Iwasa, Superconductivity in a chiral nanotube, Nat. Commun. **8**, 14465 (2017).

[8] K. Yasuda, H. Yasuda, T. Liang, R. Yoshimi, A. Tsukazaki, K. S. Takahashi, N. Nagaosa, M. Kawasaki, and Y. Tokura, Nonreciprocal charge transport at topological insulator/superconductor interface, Nat. Commun. **10**, 2734 (2019).

[9] E. Zhang, X. Xu, Y.-C. Zou, L. Ai, X. Dong, C. Huang, P. Leng, S. Liu, Y. Zhang, Z. Jia, X. Peng, M. Zhao, Y. Yang, Z. Li, H. Guo, S. J. Haigh, N. Nagaosa, J. Shen, and F. Xiu, Nonreciprocal superconducting $NbSe_2$ antenna, Nat. Commun. **11**, 5634 (2020).

[10] F. Ando, Y. Miyasaka, T. Li, J. Ishizuka, T. Arakawa, Y. Shiota, T. Moriyama, Y. Yanase, and T. Ono, Observation of superconducting diode effect, Nature (London) **584**, 373 (2020).

[11] Y.-Y. Lyu, J. Jiang, Y.-L. Wang, Z.-L. Xiao, S. Dong, Q.-H. Chen, M. V. Milošević, H. Wang, R. Divan, J. E. Pearson, P. Wu, F. M. Peeters, and W.-K. Kwok, Superconducting diode effect via conformal-mapped nanoholes, Nat. Commun. **12**, 2703 (2021).

[12] H. Wu, Y. Wang, Y. Xu, P. K. Sivakumar, C. Pasco, U. Filippozzi, S. S. P. Parkin, Y.-J. Zeng, T. McQueen, and M. N. Ali, The field-free Josephson diode in a van der Waals heterostructure, Nature (London) **604**, 653 (2022).

[13] C. Baumgartner, L. Fuchs, A. Costa, S. Reinhardt, S. Gronin, G. C. Gardner, T. Lindemann, M. J. Manfra, P. E. Faria Junior, D. Kochan, J. Fabian, N. Paradiso, and C. Strunk, Supercurrent rectification and magnetochiral effects in symmetric Josephson junctions, Nat. Nanotechnol. **17**, 39 (2022).

[14] L. Bauriedl, C. Bäuml, L. Fuchs, C. Baumgartner, N. Paulik, J. M. Bauer, K.-Q. Lin, J. M. Lupton, T. Taniguchi, K. Watanabe, C. Strunk, and N. Paradiso, Supercurrent diode effect and magnetochiral anisotropy in few-layer $NbSe_2$, Nat. Commun. **13**, 4266 (2022).

[15] J.-X. Lin, P. Siriviboon, H. D. Scammell, S. Liu, D. Rhodes, K. Watanabe, T. Taniguchi, J. Hone, M. S. Scheurer, and J. I. A. Li, Zero-field superconducting diode effect in small-twist-angle trilayer graphene, Nat. Phys. **18**, 1221 (2022).

[16] H. Narita, J. Ishizuka, R. Kawarazaki, D. Kan, Y. Shiota, T. Moriyama, Y. Shimakawa, A. V. Ognev, A. S. Samardak, Y. Yanase, and T. Ono, Field-free superconducting diode effect in noncentrosymmetric superconductor/ferromagnet multilayers, Nat. Nanotechnol. **17**, 823 (2022).

[17] A. Mizuno, Y. Tsuchiya, S. Awaji, and Y. Yoshida, Rectification at various temperatures in $YBa_2Cu_3O_y$ coated conductors with $PrBa_2Cu_3O_y$ buffer layers, IEEE Trans. Appl. Supercond. **32**, 1 (2022).

[18] T. Ideue and Y. Iwasa, One-way supercurrent achieved in an electrically polar film, Nature (London) **584**, 349 (2020).

[19] N. F. Q. Yuan and L. Fu, Supercurrent diode effect and finite momentum superconductors, Proc. Natl. Acad. Sci. USA **119**, e2119548119 (2022).

[20] A. Daido, Y. Ikeda, and Y. Yanase, Intrinsic superconducting diode effect, Phys. Rev. Lett. **128**, 037001 (2022).

[21] J. J. He, Y. Tanaka, and N. Nagaosa, A phenomenological theory of superconductor diodes, New J. Phys. **24**, 053014 (2022).

[22] S. Ilić and F. S. Bergeret, Theory of the supercurrent diode effect in Rashba superconductors with arbitrary disorder, Phys. Rev. Lett. **128**, 177001 (2022).
[23] J. J. He, Y. Tanaka, and N. Nagaosa, The supercurrent diode effect and nonreciprocal paraconductivity due to the chiral structure of nanotubes, Nat. Commun. **14**, 3330 (2023).
[24] Z. Z. Du, H.-Z. Lu, and X. C. Xie, Nonlinear Hall effects, Nat. Rev. Phys. **3**, 744 (2021).
[25] I. Sodemann and L. Fu, Quantum nonlinear Hall effect induced by Berry curvature dipole in time-reversal invariant materials, Phys. Rev. Lett. **115**, 216806 (2015).
[26] Q. Ma, S.-Y. Xu, H. Shen, D. MacNeill, V. Fatemi, T.-R. Chang, A. M. Mier Valdivia, S. Wu, Z. Du, C.-H. Hsu, S. Fang, Q. D. Gibson, K. Watanabe, T. Taniguchi, R. J. Cava, E. Kaxiras, H.-Z. Lu, H. Lin, L. Fu, N. Gedik *et al.*, Observation of the nonlinear Hall effect under time-reversal-symmetric conditions, Nature (London) **565**, 337 (2019).
[27] K. Kang, T. Li, E. Sohn, J. Shan, and K. F. Mak, Nonlinear anomalous Hall effect in few-layer WTe_2, Nat. Mater. **18**, 324 (2019).
[28] D. Kumar, C.-H. Hsu, R. Sharma, T.-R. Chang, P. Yu, J. Wang, G. Eda, G. Liang, and H. Yang, Room-temperature nonlinear Hall effect and wireless radiofrequency rectification in Weyl semimetal $TaIrTe_4$, Nat. Nanotechnol. **16**, 421 (2021).
[29] Y. M. Itahashi, T. Ideue, S. Hoshino, C. Goto, H. Namiki, T. Sasagawa, and Y. Iwasa, Giant second harmonic transport under time-reversal symmetry in a trigonal superconductor, Nat. Commun. **13**, 1659 (2022).
[30] Y. Zhang and L. Fu, Terahertz detection based on nonlinear Hall effect without magnetic field, Proc. Natl. Acad. Sci. USA **118**, e2100736118 (2021).
[31] R. Toshio and N. Kawakami, Plasmonic quantum nonlinear Hall effect in noncentrosymmetric two-dimensional materials, Phys. Rev. B **106**, L201301 (2022).
[32] R. Wakatsuki and N. Nagaosa, Nonreciprocal current in noncentrosymmetric Rashba superconductors, Phys. Rev. Lett. **121**, 026601 (2018).
[33] S. Hoshino, R. Wakatsuki, K. Hamamoto, and N. Nagaosa, Nonreciprocal charge transport in two-dimensional noncentrosymmetric superconductors, Phys. Rev. B **98**, 054510 (2018).
[34] Y. Wu, Q. Wang, X. Zhou, J. Wang, P. Dong, J. He, Y. Ding, B. Teng, Y. Zhang, Y. Li, C. Zhao, H. Zhang, J. Liu, Y. Qi, K. Watanabe, T. Taniguchi, and J. Li, Nonreciprocal charge transport in topological kagome superconductor CsV_3Sb_5, npj Quantum Mater. **7**, 105 (2022).
[35] C. Guo, C. Putzke, S. Konyzheva, X. Huang, M. Gutierrez-Amigo, I. Errea, D. Chen, M. G. Vergniory, C. Felser, M. H. Fischer, T. Neupert, and P. J. W. Moll, Switchable chiral transport in charge-ordered kagome metal CsV_3Sb_5, Nature (London) **611**, 461 (2022).
[36] E. Bauer and M. Sigrist, *Non-Centrosymmetric Superconductors: Introduction and Overview* (Springer Science + Business Media, New York, 2012).
[37] M. Smidman, M. B. Salamon, H. Q. Yuan, and D. F. Agterberg, Superconductivity and spin-orbit coupling in noncentrosymmetric materials: A review, Rep. Prog. Phys. **80**, 036501 (2017).
[38] D. F. Agterberg, Novel magnetic field effects in unconventional superconductors, Physica C **387**, 13 (2003).
[39] V. Barzykin and L. P. Gor'kov, Inhomogeneous stripe phase revisited for surface superconductivity, Phys. Rev. Lett. **89**, 227002 (2002).
[40] O. V. Dimitrova and M. V. Feigel'man, Phase diagram of a surface superconductor in parallel magnetic field, JETP Lett. **78**, 637 (2003).
[41] R. P. Kaur, D. F. Agterberg, and M. Sigrist, Helical vortex phase in the noncentrosymmetric $CePt_3Si$, Phys. Rev. Lett. **94**, 137002 (2005).
[42] D. F. Agterberg and R. P. Kaur, Magnetic-field-induced helical and stripe phases in Rashba superconductors, Phys. Rev. B **75**, 064511 (2007).
[43] O. Dimitrova and M. V. Feigel'man, Theory of a two-dimensional superconductor with broken inversion symmetry, Phys. Rev. B **76**, 014522 (2007).
[44] K. V. Samokhin, Upper critical field in noncentrosymmetric superconductors, Phys. Rev. B **78**, 224520 (2008).
[45] Y. Yanase and M. Sigrist, Helical superconductivity in noncentrosymmetric superconductors with dominantly spin triplet pairing, J. Phys. Soc. Jpn. **77**, 342 (2008).
[46] K. Michaeli, A. C. Potter, and P. A. Lee, Superconducting and ferromagnetic phases in $SrTiO_3/LaAlO_3$ oxide interface structures: Possibility of finite momentum pairing, Phys. Rev. Lett. **108**, 117003 (2012).
[47] M. Houzet and J. S. Meyer, Quasiclassical theory of disordered Rashba superconductors, Phys. Rev. B **92**, 014509 (2015).
[48] P. Fulde and R. A. Ferrell, Superconductivity in a strong spin-exchange field, Phys. Rev. **135**, A550 (1964).
[49] A. I. Larkin and Y. N. Ovchinnikov, Nonuniform state of superconductors, Zh. Eksp. Teor. Fiz. **47**, 1136 (1964).
[50] Y. Matsuda and H. Shimahara, Fulde–Ferrell–Larkin–Ovchinnikov state in heavy fermion superconductors, J. Phys. Soc. Jpn. **76**, 051005 (2007).
[51] J. Wosnitza, FFLO states in layered organic superconductors, Ann. Phys. (Berlin) **530**, 1700282 (2018).
[52] D. F. Agterberg, J. C. S. Davis, S. D. Edkins, E. Fradkin, D. J. Van Harlingen, S. A. Kivelson, P. A. Lee, L. Radzihovsky, J. M. Tranquada, and Y. Wang, The physics of pair-density waves: Cuprate superconductors and beyond, Annu. Rev. Condens. Matter Phys. **11**, 231 (2020).
[53] K. Kumagai, H. Shishido, T. Shibauchi, and Y. Matsuda, Evolution of paramagnetic quasiparticle excitations emerged in the high-field superconducting phase of $CeCoIn_5$, Phys. Rev. Lett. **106**, 137004 (2011).
[54] H. Mayaffre, S. Krämer, M. Horvatić, C. Berthier, K. Miyagawa, K. Kanoda, and V. F. Mitrović, Evidence of Andreev bound states as a hallmark of the FFLO phase in κ-(BEDT-TTF)$_2$Cu(NCS)$_2$, Nat. Phys. **10**, 928 (2014).
[55] G. Koutroulakis, H. Kühne, J. A. Schlueter, J. Wosnitza, and S. E. Brown, Microscopic study of the Fulde-Ferrell-Larkin-Ovchinnikov state in an all-organic superconductor, Phys. Rev. Lett. **116**, 067003 (2016).
[56] S. Kitagawa, G. Nakamine, K. Ishida, H. S. Jeevan, C. Geibel, and F. Steglich, Evidence for the presence of the Fulde-Ferrell-Larkin-Ovchinnikov state in $CeCu_2Si_2$ revealed using ^{63}Cu NMR, Phys. Rev. Lett. **121**, 157004 (2018).
[57] S. Kasahara, H. Suzuki, T. Machida, Y. Sato, Y. Ukai, H. Murayama, S. Suetsugu, Y. Kasahara, T. Shibauchi, T. Hanaguri, and Y. Matsuda, Quasiparticle nodal plane in the

Fulde-Ferrell-Larkin-Ovchinnikov state of FeSe, Phys. Rev. Lett. **127**, 257001 (2021).

[58] K. Kinjo, M. Manago, S. Kitagawa, Z. Q. Mao, S. Yonezawa, Y. Maeno, and K. Ishida, Superconducting spin smecticity evidencing the Fulde-Ferrell-Larkin-Ovchinnikov state in Sr_2RuO_4, Science **376**, 397 (2022).

[59] M. H. Hamidian, S. D. Edkins, S. H. Joo, A. Kostin, H. Eisaki, S. Uchida, M. J. Lawler, E.-A. Kim, A. P. Mackenzie, K. Fujita, J. Lee, and J. C. S. Davis, Detection of a Cooper-pair density wave in $Bi_2Sr_2CaCu_2O_{8+x}$, Nature (London) **532**, 343 (2016).

[60] W. Ruan, X. Li, C. Hu, Z. Hao, H. Li, P. Cai, X. Zhou, D.-H. Lee, and Y. Wang, Visualization of the periodic modulation of cooper pairing in a cuprate superconductor, Nat. Phys. **14**, 1178 (2018).

[61] H. Chen, H. Yang, B. Hu, Z. Zhao, J. Yuan, Y. Xing, G. Qian, Z. Huang, G. Li, Y. Ye, S. Ma, S. Ni, H. Zhang, Q. Yin, C. Gong, Z. Tu, H. Lei, H. Tan, S. Zhou, C. Shen *et al.*, Roton pair density wave in a strong-coupling kagome superconductor, Nature (London) **599**, 222 (2021).

[62] Q. Gu, J. P. Carroll, S. Wang, S. Ran, C. Broyles, H. Siddiquee, N. P. Butch, S. R. Saha, J. Paglione, J. C. S. Davis, and X. Liu, Detection of a pair density wave state in UTe_2, Nature (London) **618**, 921 (2023).

[63] A. Daido and Y. Yanase, Superconducting diode effect and nonreciprocal transition lines, Phys. Rev. B **106**, 205206 (2022).

[64] Y. Kim, M. J. Park, and M. J. Gilbert, Probing unconventional superconductivity in inversion-symmetric doped Weyl semimetal, Phys. Rev. B **93**, 214511 (2016).

[65] M. Tinkham, J. U. Free, C. N. Lau, and N. Markovic, Hysteretic *I-V* curves of superconducting nanowires, Phys. Rev. B **68**, 134515 (2003).

[66] Y. Hou, F. Nichele, H. Chi, A. Lodesani, Y. Wu, M. F. Ritter, D. Z. Haxell, M. Davydova, S. Ilić, O. Glezakou-Elbert, A. Varambally, F. S. Bergeret, A. Kamra, L. Fu, P. A. Lee, and J. S. Moodera, Ubiquitous superconducting diode effect in superconductor thin films, Phys. Rev. Lett. **131**, 027001 (2023).

[67] D. Y. Vodolazov and F. M. Peeters, Superconducting rectifier based on the asymmetric surface barrier effect, Phys. Rev. B **72**, 172508 (2005).

[68] M. Naritsuka, T. Ishii, S. Miyake, Y. Tokiwa, R. Toda, M. Shimozawa, T. Terashima, T. Shibauchi, Y. Matsuda, and Y. Kasahara, Emergent exotic superconductivity in artificially engineered tricolor Kondo superlattices, Phys. Rev. B **96**, 174512 (2017).

[69] M. Naritsuka, T. Terashima, and Y. Matsuda, Controlling unconventional superconductivity in artificially engineered *f*-electron Kondo superlattices, J. Phys.: Condens. Matter **33**, 273001 (2021).

[70] T. Sekihara, R. Masutomi, and T. Okamoto, Two-dimensional superconducting state of monolayer Pb films grown on GaAs(110) in a strong parallel magnetic field, Phys. Rev. Lett. **111**, 057005 (2013).

[71] T. Schumann, L. Galletti, H. Jeong, K. Ahadi, W. M. Strickland, S. Salmani-Rezaie, and S. Stemmer, Possible signatures of mixed-parity superconductivity in doped polar $SrTiO_3$ films, Phys. Rev. B **101**, 100503(R) (2020).

[72] A. Larkin and A. Varlamov, *Theory of Fluctuations in Superconductors* (Oxford University Press, Oxford, 2005).

[73] See Supplemental Material at http://link.aps.org/supplemental/10.1103/PhysRevResearch.6.L022009 for more details.

[74] A. Schmid, Diamagnetic susceptibility at the transition to the superconducting state, Phys. Rev. **180**, 527 (1969).

[75] F. Konschelle, J. Cayssol, and A. I. Buzdin, Anomalous fluctuation regimes at FFLO transition, Europhys. Lett. **79**, 67001 (2007).

[76] A. T. Bollinger, G. Dubuis, J. Yoon, D. Pavuna, J. Misewich, and I. Božović, Superconductor-insulator transition in $La_{2-x}Sr_xCuO_4$ at the pair quantum resistance, Nature (London) **472**, 458 (2011).

[77] X. Leng, J. Garcia-Barriocanal, S. Bose, Y. Lee, and A. M. Goldman, Electrostatic control of the evolution from a superconducting phase to an insulating phase in ultrathin $YBa_2Cu_3O_{7-x}$ films, Phys. Rev. Lett. **107**, 027001 (2011).

[78] T. Nojima, H. Tada, S. Nakamura, N. Kobayashi, H. Shimotani, and Y. Iwasa, Hole reduction and electron accumulation in $YBa_2Cu_3O_y$ thin films using an electrochemical technique: Evidence for an *n*-type metallic state, Phys. Rev. B **84**, 020502(R) (2011).

[79] M. Liao, Y. Zhu, J. Zhang, R. Zhong, J. Schneeloch, G. Gu, K. Jiang, D. Zhang, X. Ma, and Q.-K. Xue, Superconductor-insulator transitions in exfoliated $Bi_2Sr_2CaCu_2O_{8+\delta}$ flakes, Nano Lett. **18**, 5660 (2018).

[80] E. Abrahams and T. Tsuneto, Time variation of the Ginzburg-Landau order parameter, Phys. Rev. **152**, 416 (1966).

[81] T. Asaba and Y. Matsuda (private communication).